Adsorption of Carotene from Crude Palm Oil by Activated Achalla Clay

Ajemba, Regina O. [a], Nweke Chinenyenwa N. [a*], Okoye Chisom C. [a] and Nwachukwu Josiah O. [b]

[a] *Department of Chemical Engineering, Faculty of Engineering, Nnamdi Azikiwe University, P.M.B. 5025, Awka, Anambra State, Nigeria.*
[b] *Department of Civil Engineering, Faculty of Engineering, Nnamdi Azikiwe University, P.M.B. 5025, Awka, Anambra State, Nigeria.*

Authors' contributions

This work was carried out in collaboration among all authors. All authors read and approved the final manuscript.

Original Research Article

ABSTRACT

High costs of imported bleaching earths have led to the need for alternative local sources. The effectiveness of acid-activated Achalla clay in crude palm oil bleaching was examined. The clay sample was collected, sun-dried, manually ground, and activated with the hydrochloric acid solution. Characterization of the raw and activated clay samples was carried out using X-ray fluorescence (XRF), Scanning electron microscopy (SEM), and Fourier transform infrared spectroscopy (FTIR) analyses. The factors that were varied during the bleaching process were temperature, contact time, and adsorbent dosage. The adsorption kinetics, adsorption isotherm, and thermodynamics studies were also investigated. The XRF, SEM, and FTIR characterization results showed that the clays were kaolinites with some significant increase in the number of microporous surfaces and some changes in the functional groups. The results also indicated that the process performance improved at higher temperatures. The highest bleaching efficiency of the bleaching process was 85.6%. The pseudo-first-order model described the adsorption process from the experimental data with higher correlation coefficients than the pseudo-second-order, first-order,

---

*Corresponding author: Email: cn.nweke@unizik.edu.ng;

and Intra-particle diffusion models. The equilibrium isotherm data were described better by the Temkin model than Langmuir and Freundlich models due to higher R^2 values. The enthalpy and entropy values were determined to be 26,968.12 J/mol and 78.2273 J/mol respectively. The Gibb's free energy was found to vary between -1.428.39 to 1,700.70 J/mol. The results of the thermodynamic parameters showed that it was a spontaneous chemical adsorption process and endothermic. This study has revealed that acid-activated Achalla clay can be used for the bleaching of crude palm oil at higher temperatures.

1. INTRODUCTION

Palm oil is an important oil crop in Nigeria. It is used in producing food and household products like margarine, shortenings, cooking oils, confectionery fats, and soaps. It can also be added to fuel in some engines [1]. "However, the reddish color of palm oil is due to its high β-carotene content and its removal is highly important to obtain its commercial qualities which include light color, good oxidative stability, and bland taste" [2]. "This is because raw palm oil contains impurities like oxidation metals, organic pigments, trace metals, and trace soaps" [3].

"To make palm oil edible, these impurities which negatively influence the taste, smell, appearance, and shelf-life stability of the oil, thereby reducing its acceptance and marketability by the consumer need to be removed. Chemical and physical refining techniques can both be used for palm oil processing" [4]. "Physical refinery which is the most commonly applied in palm oil treatment consists of degumming, bleaching, and deodorization steps" [3]. "Chemical techniques involve acid degumming, alkali refining, bleaching, deodorization, and winterization stages" [4].

"Bleaching, which is the most critical process, removes a part of the color pigments, oxidation products, and minor constituents while deodorization thermally degrades the remaining pigments at high temperatures" [2]. "These color pigments produced by compounds include carotene, carotenoids, chlorophyll, and xanthophylls present in palm oil" [5]. "Hence, refining crude palm oil through adsorptive bleaching with the use of adsorbents remains very important and necessary for the removal of pigments and other unwanted compounds which negatively influence the taste of the oil. This is done by bringing the oil into contact with a surface-active substance that adsorbs the undesired particles" [3].

"Bleaching of palm oil is been carried out with the use of activated carbons and activated bleaching earth" [6,3,7]. "The bleaching earth is also known as acid-activated clays while Fuller's earth is raw clays" [4]. "It is well known that clay minerals can be used to decolorize oils because of their high adsorptive capacity. In other to enhance this adsorptive property, acid activation of clay is the most commonly used technique. Many factors have been reported to influence the bleaching performance of activated clay; these include the mineralogical and chemical composition of the clay, the clay's particle size, the type and concentration of the activating agent, activation temperature, bleaching temperature, bleaching time, clay dosage, moisture content" [4,5].

"The knowledge of adsorption kinetics and equilibrium adsorption isotherm studies on an adsorbate–adsorbent system is important in the design of adsorption treatment plants. The relationship between the adsorbate concentration and adsorbent as a function of time is described by adsorption kinetics and aids in selecting the required reactor dimensions" [8]. On the other hand, equilibrium adsorption studies describe the equilibrium conditions of the adsorption process, while considering the concentration of the adsorbate in the liquid and solid phases at a definite temperature. The results obtained from equilibrium adsorption isotherm studies give information on the capacity and affinity of the adsorbent for the adsorbate [8]. Applying the right kinetic model gives the right mechanism for the adsorption of beta-carotene and leads to the high efficiency of the process control [9].

The results from previous kinetic studies of vegetable oil bleaching showed that the effect of catalysis on bleaching earth led to the fast decomposition of long β-carotene molecules to shorter molecules [4]. Previous studies involved the bleaching of palm oil with activated clay samples and kinetic studies on the bleaching process but these studies did not investigate the

bleaching of locally prepared palm oil with local Achalla clay from Anambra State.

Hence, the goal of this work is to investigate and develop a good local substitute for the commercially imported adsorbent (fuller's earth) with the use of Achalla clay. The modification of Achalla clay sample with acid activation will be termed effective from the percentage color reduction obtained during its use in the bleaching of locally prepared palm oil. This research also investigated the adsorption kinetics and equilibrium characteristics of the activated carbon on the local palm oil bleaching using three kinetic models (pseudo-first-order, pseudo-second-order model and Intra-particle diffusion models) and three equilibrium models (Langmuir, Freundlich, and Temkin isotherm models).

2. MATERIALS AND METHODS

Detailed instruction about this section is given below:

2.1 Materials

The raw clay sample (ACC) was obtained from Achalla town, in Awka North local government (6.3367ºN, 6.9880ºE), Anambra State, Nigeria. The crude palm oil was milled locally at Ifite, Awka in Anambra State. Other materials included hydrochloric acid (JHD, China), acetone (BDH, England), and distilled water (Springboard, Nigeria).

2.2 Clay Preparation

The clay sample obtained was sun-dried for 24 hours to make them amenable to grinding. It was then ground with a local mortar and pestle and sieved using a 150 μm mesh size.

2.3 Degumming

500 mL of crude palm oil was measured into a 2000 mL beaker and 1000 mL of boiled water was added to it. The gums and water were separated from the hot oil using a separating funnel. The process was repeated twice to ensure thorough removal of all the hydratable gums.

2.4 Acid Activation

200 g of the raw clay sample (ACC) was measured and mixed thoroughly with 250 mL of 5 M concentration of hydrochloric acid (HCl) to form a slurry. The mixture was put into a 500 mL beaker. The slurry was heated with a magnetic stirred hot plate (Adarsh, India) at 100 ^{o}C for 2 hours while being continuously stirred. After the acid activation, the slurry was allowed to cool in the air at room temperature. The slurry was filtered and washed free of acid (to pH ≈ 7) with distilled water. The acid-activated Achalla clay (AACC) was then dried at a temperature of 105 ^{o}C for 24 hours in the oven (Memmert, England). It was later ground using mortar and pestle, sieved using 150 μm mesh/sieve size, and stored for subsequent use.

2.5 Clay Characterization

The characterization carried out on the clays are explained below.

2.5.1 X-ray fluorescence (XRF) analysis

The chemical compositions of the clay sample before and after activation were determined using X-supreme8000 XRF spectrometer, China.

2.5.2 Fourier transform infrared spectroscopy (FTIR) analysis

FTIR analysis of the clay sample before and after activation was carried out using a Shimadzu FTIR-8400S spectrophotometer, Europe. All FT-IR spectra were recorded in the range of 4000-400 cm^{-1}.

2.5.3 Scanning electron microscopy (SEM) analysis

A scanning electron microscope (Phenom ProX, Netherlands) was used to evaluate the surface morphology of the clay sample before and after activation.

2.6 Adsorption Kinetics Experiment

The batch process was applied in carrying out the bleaching experiment. 100 mL of the crude palm oil was measured into a 500 mL beaker and placed on a hot plate to reach the desired temperature before adding 1.0 g of AACC. The sample was continuously stirred during the bleaching period. The sample contained in the beaker was taken from the hot plate at the respective time of 10, 20, 30, 40, 45, and 50 mins and filtered to measure the absorbance using a UV spectrophotometer [3]. The experiments were carried out at temperatures of 50, 70, 90, and 100 ^{o}C. The effect of contact time on the bleaching efficiency of AACC was tested with four kinetic models. The mechanism

controlling the adsorption process was evaluated using the intra-particle diffusion model [10].

2.6.1 First-order model

The model equation assumes that the digestion process followed first-order and is given as [11],

$$lnC_t = \frac{k_1 t}{C_o} \tag{1}$$

2.6.2 Pseudo-first-order model

The model evaluates the removal mechanism of β-carotene as adsorption is carried out through a boundary by diffusion. The model assumes that the adsorption of one adsorbate molecule took place onto one active site on the adsorbent surface [8]. The linear equation is given as

$$\ln(q_e - q_t) = \ln q_e - K_1 t \tag{2}$$

where q_e and q_t are the amount of β-carotene adsorbed (mg/g) at equilibrium and at time t (min), respectively, and K_1 (min^{-1}) is the pseudo-first-order rate constant. The model predicted q_e and K_1 are evaluated from the intercept and slope respectively from the plot of $\ln(q_e - q_t)$ against time (t) [10,3].

2.6.3 Pseudo-second-order model

The model equation is based on the assumption that the adsorption of one adsorbate molecule took place on two active sites of the adsorbent surface [8]. The model is focused on the adsorption capacity of the solid phase [12]. The linear equation is given as

$$\frac{t}{q_t} = \frac{1}{K_2 q_e^2} + t\left(\frac{1}{q_e}\right) \tag{3}$$

where qe and qt are the amounts of β-carotene adsorbed (mg/g) at equilibrium and at time t (min), respectively, and K_2 (g/mg min) is the pseudo-second-order rate constant. The Pseudo-second order rate constant K_2, and qe were determined from the slope and intercept of the plot of $^t/_{q_t}$ versus t respectively [10].

2.6.4 Intra-particle diffusion model

This model is applied from a mechanistic viewpoint [8]. The linear form of the equation [10] is

$$q_t = K_d t^{0.5} + \varepsilon \tag{4}$$

where qt is the amount of β-carotene adsorbed per unit weight of the adsorbent, ε (mg/g) is a constant which gives information about the boundary layer and K_d (mg/g min$^{-1/2}$) is the intraparticle diffusion rate constant and t is the contact time. A plot of q_t against t$^{1/2}$ gives the slope, K_d and the intercept, ε respectively.

2.7 Equilibrium Adsorption Studies

The bleaching vessels were 500 mL beakers which were placed on a hot plate. The palm oil (100 mL) was heated to the desired temperature before the clay. The mixture was continuously heated and stirred. The hot oil and clay mixture were filtered at the end of the experiment before measuring the absorbance using a UV spectrophotometer. The equilibrium adsorption experiment was carried out at different masses of the activated clay (1.0, 1.5, 2.0, 2.5, 3.0, and 7.0 g by weight). The experiments were carried out at the temperature of 100 ºC and contact times of 10, 20, 30, 40, 45, and 50 minutes. This was done to investigate the effect of mass percent of clay on the percentage decrease in absorbance of bleached palm oil.

2.8 Adsorption Isotherm Modelling

The isotherm models used for the study were as follows.

2.8.1 Langmuir model

The Langmuir isotherm model assumed that the adsorption at a particular site stops as soon as the adsorbent site is covered with the β-carotene molecules [8]. It also stipulates that all the adsorption sites have equivalent energy. The linear model equation [13,14] is given as

$$\frac{X_e}{q_e} = \frac{1}{K_1 q_m} - \frac{X_e}{q_m} \tag{5}$$

where $q_e = \frac{X}{m}$, $X = \frac{A_o - A_t}{A_o}$ and $X_e = 1 - X$ qe is the adsorption capacity of the adsorbent (mg/g) at equilibrium, m is the mass of the adsorbent (g). X is the amount of adsorbed solute while X_e is the amount of un-adsorbed solute. A_o and A are the absorbances of crude oil and bleached oil respectively. The values of slope (K_1) and intercept (q_m) represents the maximum adsorption capacity and the adsorption equilibrium constant respectively and were evaluated from the plot of $\frac{X_e}{q_e}$ against X_e. The

Langmuir adsorption isotherm model only gives information on the equilibrium process and adsorption capability of the adsorption process [8].

2.8.2 Freundlich model

The Freundlich isotherm model is based on the assumption that adsorption takes place on a heterogeneous surface [8]. The nonlinear expression of the Freundlich equation [13] is given as

$$log\ q_e = \log K + \frac{1}{n} log\ X_e \qquad (6)$$

where K is a measure of the adsorption capacity while n is the heterogeneity factor and a measure of the intensity of adsorption [10]. The slope (*log K*) and intercept (*1/n*) were evaluated from the plot of log q_e (*X/m*) against log X_e respectively. The larger the value of the adsorption capacity K, the higher the adsorption capacity. The magnitude of *1/n* in the ranges between 0 and 1 indicates favorable adsorption and as its value tends to zero, it becomes more heterogeneous. The Freundlich model equation is characterized by multilayer adsorption [8].

2.8.3 Temkin model

This model deals with the indirect interactions between the adsorbent and the adsorbate that occur during the coverage of the surface resulting in a linear decrease in the heat of adsorption [15,16]. It does not assume a saturation limit [16]. The linear form of the Temkin model is given as

$$q_e = B_1 ln K_T + B_1 ln X_e \qquad (7)$$

where $B_1 = \frac{RT}{b}$, R is the ideal gas constant (8.314 J/mol K), T is the temperature in Kelvin, K_T (mg/g) is the Temkin isotherm equilibrium binding constant corresponding to the maximum binding energy and B_1 (Jmol^{-1}) is the Temkin isotherm constant that is related to the heat of adsorption, b (kJ/mol) is the adsorption energy variation, q_e ($\frac{X}{m}$) is the quantity of adsorbed color pigment at equilibrium (mg/g) and X_e (mgL^{-1}) is the equilibrium concentration at equilibrium [11,16]. The Temkin constants, K_T and B_1 are evaluated from the slope and intercept of the plot of q_e against ln X_e [15]. The slope (B_1) and the intercept ($B_1 ln K_T$) are determined from the plot of the model equation [17].

2.9 Evaluation of the Bleaching Performance

At the end of each bleaching process, the content of the beaker was filtered through a Whatman NO 1 filter paper and the concentration of the filtrate was determined. The evaluation of the amount of pigment was made with a 752 UV-Vis spectrophotometer, China. The samples were diluted in acetone to a concentration of 10% (v/v) and the absorbance of the sample was determined at a wavelength of 450 nm using a UV spectrophotometer [3]. To measure the absorbance of the unbleached palm oil (A_0), 5 ml of the unbleached oil was diluted in acetone to a concentration of 10% (v/v), of oil to acetone ratio, and its absorbance was determined at a wavelength of 450 nm (nanometer) using the UV spectrophotometer. The bleaching performance of the absorbent was determined from equation (7) [12].

$$\text{Bleaching performance (\%)} = \frac{A_o - A_t}{A_0} \times 100\% \qquad (8)$$

Where A_0 and A_t are the absorbances of crude oil and bleached oil at time, *t* respectively.

2.10 Adsorption Thermodynamics

Adsorption thermodynamics studies can be used to give detailed information on the intrinsic energy and structural changes after adsorption [14]. Both energy and entropy factors are considered necessary when determining whether the adsorption process occurred spontaneously or not [14,6]. The properties of thermodynamics properties being Gibbs free energy change (ΔG^o), enthalpy change (ΔH^o), and entropy change (ΔS^o) were evaluated, all in J/mol [12,10].

$$\Delta G^o = RT ln(k_d) \qquad (9)$$

Where

ΔG^o is the Gibbs free energy change of adsorption, R is the universal gas constant (8.314 Jmol^{-1}K^{-1}), T is the absolute temperature (K) and k_d is the thermodynamic equilibrium constant. k_d is calculated from equation (10).

$$k_d = \frac{q_e}{X_e} \qquad (10)$$

The enthalpy (ΔH^o) and entropy (ΔS^o) values are estimated from equation (11) where

$$lnk_d = \frac{\Delta S}{R} - \frac{\Delta H}{RT} \qquad (11)$$

$$\Delta G = \Delta H - T\Delta S \qquad (12)$$

The values of ΔG° were calculated from Equation (12) [14,15]. The values of ΔH° and ΔS° were calculated from the slope and intercept of the plot of ln k_d versus 1/T. ΔG° evaluates whether the process was a feasible and spontaneous one or not, ΔH° determines if the process was exothermic or endothermic, whereas ΔS° showed the random increase or decrease of the process at the solid/solution interface. A spontaneous reaction is obtained where a negative value of ΔG° is obtained [10]. The evaluation of the thermodynamic studies was carried out using the absorbance values obtained from the adsorption kinetics experiment.

3. RESULTS AND DISCUSSION

3.1 Characterization of the Adsorbent

The results of the characterization of the clay samples are as follows:

3.1.1 Fourier transform infrared spectroscopy (FTIR) analysis of the adsorbents

"The infrared spectra were obtained for the adsorbents before and after the activation process with 5M HCl at 100 °C for 2 hours in a wavenumber range of 4000 – 650 cm^{-1}. The FTIR results of the raw and acid-activated clay samples were assigned according to the functional groups reported by" [11,18-20]. The

FTIR results revealed that some of the functional groups disappeared whereas some groups appeared after the clay activation. The changes in these functional groups could be attributed to the action of heat and acid treatment during acid activation [11]. From observation, the functional groups that significantly made up the adsorbent's compound were hydroxide (O–H), isothiocyanate (–NCS), and aromatics (C–H). The O–H stretching vibrations were observed within 3700 and 3600 cm^{-1}. The C–H for the aromatics were both in-plane bend (found within 998.8 – 1114.5 cm^{-1}) and out-of-plane bend (positioned within 670.9 -790.2 cm^{-1}). Isothiocyanate (–NCS) bond was found at 2057.5 cm^{-1} while Vinyl C–H out of plane bend was observed at 909.5 cm^{-1} [11,18-20].

The adsorbent spectra before and after the acid activation process were quite similar as also obtained in [12]. After the acid activation process, the intensity of the band in the region of 2053.8 to 998.9 cm^{-1} became increased indicating the release of water from the clay's natural humidity due to heating [12]. The wavelength in the range of 3698 cm^{-1} as obtained in both activated and raw Achalla clays indicated that both clays are characteristics of pure kaolinites ($Al_2(SiO_5)(OH)_4$) [21,22]. The dominant presence of kaolinite mineral was detected by the relative intensity of O–H stretching bands in the FTIR spectrum [23]. The kaolinite structure of the raw and activated adsorbents was partially ordered since the individual O–H bands at 3693.8, 3652.8, and 3623.0 cm^{-1} had low intensities but were identified [23]. The FTIR results for ACC and ACAC are shown in Figs. 1 and 2 respectively.
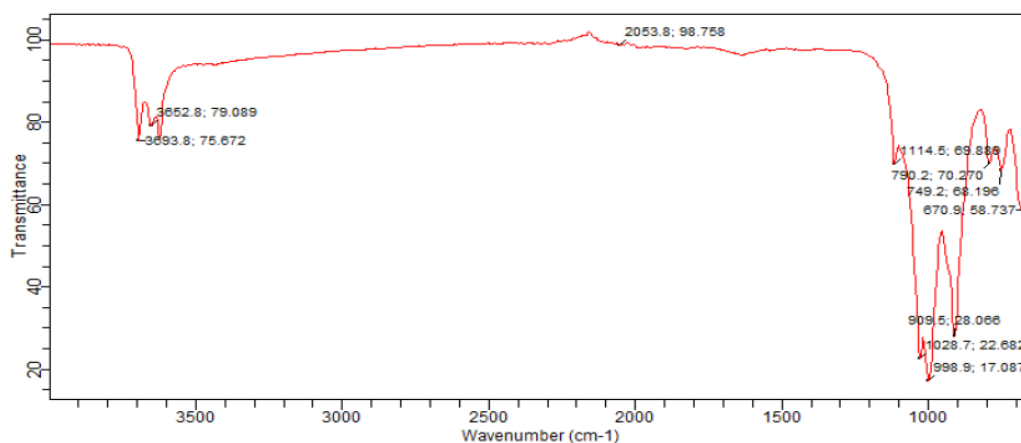

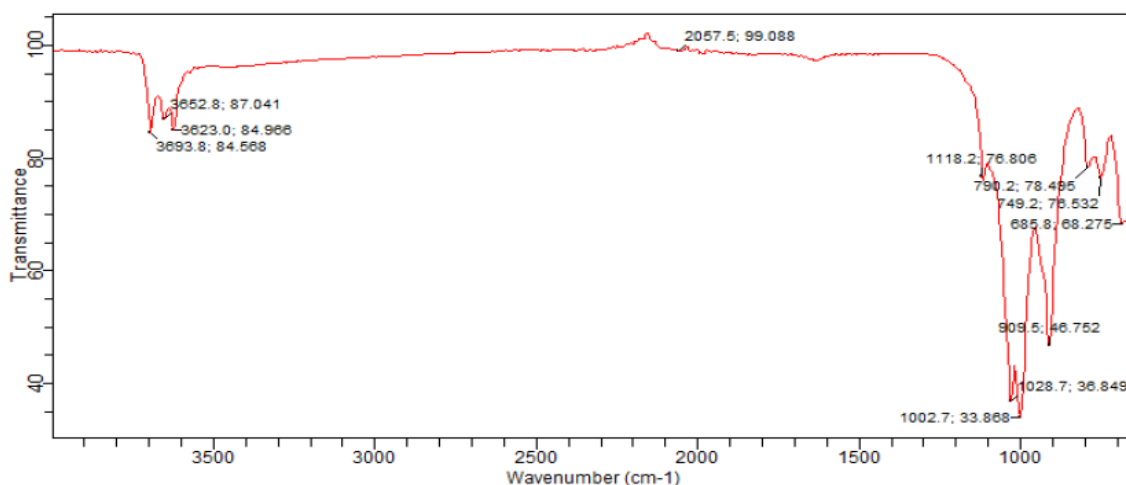**Fig. 1. FTIR spectra of raw Achalla clay (ACC)**

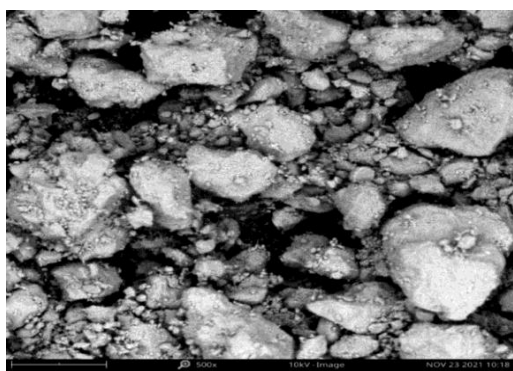**Fig. 2. FTIR spectra of acid-activated Achalla clay (ACAC)**

Fig. 3. SEM images of raw Achalla clay (ACC) (@100 μm)

3.1.2 Scanning electron microscopy (SEM) analysis of the adsorbents

SEM analysis was carried out to study the morphological properties and surface topography of the adsorbents before and after acid activation. The SEM results of ACC and ACAC are shown in Figs. 3 and 4 respectively. It was observed that there were differences in the morphology of the two clays. The particles that constituted both clays were not of the same sizes and shapes and revealed a total change in the texture of the surface of the activated clay. This was in consistence with previous results [8]. The result from ACC showed that there was a smooth surface morphology with pores of different sizes of crystallites in addition to luminous and non-luminous outlines confirming the presence of inorganic and organic materials. This was similar to the results obtained by some researchers [11,24]. The result showed that ACAC was loosely packed and coarse, as also seen in [25]. There were more pore spaces in ACAC than in ACC. This was in consistence with results obtained in [24]. It was observed that the particles of the raw clay were not of regular sizes and shapes but became more finely shaped after acid activation. Since adsorption is a surface reaction, an increment of pore spaces favors the bleaching process. The SEM analysis results indicated coarsely and loosely packs surfaces with irregular and hexagonal edges confirming that the clays were kaolinites. This observation was also reported by [25].

3.1.3 X-ray Fluorescence (XRF) analysis of the adsorbents

The XRF results of the oxides and elements in ACC and ACAC are shown in Tables 1 and 2 respectively.

Fig. 4. SEM images of acid-activated Achalla clay (ACAC) (@100 μm)

Table 1. XRF result of oxides from raw and activated Achalla clays

Oxide	Concentration of raw Achalla clay (%)	Concentration of acid-activated Achalla clay (%)
SiO_2	64.292	74.800
V_2O_5	0.073	0.052
Cr_2O_3	0.011	0.017
MnO	0.013	0.035
Fe_2O_3	7.914	1.309
CO_3O_4	0.023	0.002
NiO	0.002	0.006
CuO	0.045	0.034
Nb_2O_3	0.010	0.007
MoO_3	0.003	0.001
WO_3	0.001	0.000
P_2O_5	0.000	0.027
SO_3	0.118	0.008
CaO	0.474	0.454
MgO	1.237	0.000
K_2O	0.289	0.228
BaO	0.000	0.010
Al_2O_3	20.685	17.681
Ta_2O_5	0.002	0.005
TiO_2	2.999	3.014
ZnO	0.009	0.004
Ag_2O	0.005	0.007
Cl	1.461	1.806
ZrO_2	0.202	0.241
SnO_2	0.000	0.000
PbO	0.017	0.004
Rb_2O	0.003	0.001
SrO	0.012	0.004

Table 2. XRF result of element from raw and activated Achalla clays

Element	Concentration of raw Achalla clay (%)	Concentration of acid-activated Achalla clay (%)
O	46.466	49.609
Mg	0.390	0.000
Al	14.48	13.722
Si	23.424	30.213
P	0.000	0.241
S	0.049	0.004
Cl	0.672	0.921
K	0.293	0.256
Ca	0.247	0.262
Ti	1.863	2.076
V	0.097	0.077
Cr	0.014	0.026
Mn	0.080	0.028
Fe	11.466	2.103
CO	0.052	0.006
Ni	0.002	0.005
Cu	0.037	0.031
Zn	0.008	0.004
Rb	0.006	0.002
Sr	0.013	0.005

Element	Concentration of raw Achalla clay (%)	Concentration of acid-activated Achalla clay (%)
Zr	0.239	0.316
Nb	0.023	0.018
MO	0.004	0.001
Ag	0.014	0.022
Sn	0.000	0.000
Ba	0.000	0.020
Ta	0.011	0.024
W	0.002	0.000
Pb	0.047	0.011

The results revealed that the dominant mineral oxides present in the raw clay were silicon oxide/quartz, iron (II) oxide/hematite, and alumina at 64.292, 7.914, and 20.685% respectively. This was also observed in [13,10]. MgO, TiO_2, and Cl of the raw clay were present in minor quantities whereas the remaining minerals were present in trace quantities. The minor quantity of MgO that was found present in the raw clay disappeared after activation. The major elements in their descending order, found in the clays were Oxygen, Silicon, Aluminum, and Iron. The other elements were seen in trace quantities. The presence of these major elements in the clays also confirmed that the clays were kaolinites [26].

3.2 Effect of Process Parameters on the Bleaching Efficiency

Effects of contact time, temperature and adsorbent dosage at a constant temperature were carried out on a batch basis for the evaluation of the bleaching efficiency. The absorbance of the raw Achalla clay (ACC) was 2.50.

3.2.1 Effect of contact time

The effect of contact time (10, 20, 30, 40, 45, 50 min) on the bleaching performance of ACAC on crude palm oil was observed at 50, 70, 90, and 100 $^{\circ}$C with a constant mass of 1 g of the adsorbent. The plot of the bleaching efficiency is shown in Fig. 5. The performance of the palm oil bleaching was observed to increase quickly in the first 30 mins but slowed down as it approached 50 mins [10,3]. This observation could be due to the large surface area during the beginning of the bleaching process and the reduction of the vacant sites towards the end of the process [4,10]. "The bleaching efficiency increased when compared from the beginning of the process till the end of the contact time of 50 mins. Optimum bleaching performance of 78.8%

was obtained at 100 $^{\circ}$C after 50 min contact time. Both the percentage removal and the adsorption capacities increased with an increase in time. Equilibrium could still be reached with an increase in adsorbent or contact time. This indicated that an increase in contact time increased the rate of the bleaching performance" [11]. It can be seen that the adsorbent demonstrated a good potential for the adsorption of carotene from palm oil.
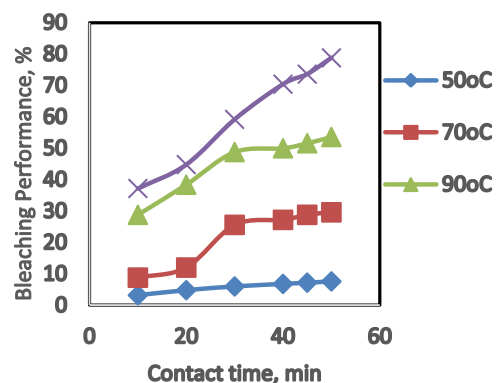

Fig. 5. Effect of contact time on the bleaching efficiency of ACAC on palm oil

3.2.2 Effect of temperature

The effect of temperature on the bleaching performance at 50, 70, 90, and 100°C with an adsorbent mass of 1 g is shown in Fig. 6. It was observed that the bleaching efficiencies of the adsorbent varied with the temperature and increased with an increase in temperature [11,3]. The highest bleaching efficiency of 78.8% was obtained at 100 $^{\circ}$C and it could be said that the optimum temperature would be obtained with an increase in temperature, contact time, or adsorbent since a lower percentage of the performance was not recorded with an increase in temperature [11]. [14] also reported an increment in bleaching efficiency as the

temperature increased up to 100 °C. The increment in temperature increased the removal of beta carotene because the rate of diffusion of oil molecules increased at the surface pores as temperature increased. With the increase in temperature, the interactions, kinetic energy, solubility, reduction in resistance to flow and adsorption of the palm oil molecules the adsorption of the oil pigments increased [11,10].
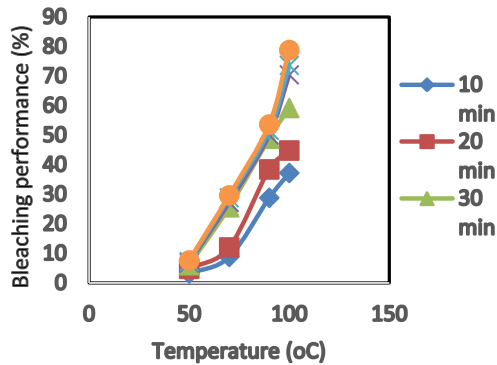

Fig. 6. Effect of temperature on the bleaching efficiency of ACAC on palm oil

3.2.3 Effect of adsorbent dosage at constant temperature

The optimum temperature obtained from the effect of temperature was found to be 100 °C. At a constant temperature of 100 °C, the mass of the adsorbent was varied from 1, 1.5, 2, 2.5, and 3 g with initial oil absorbance of 2.50 as obtained from the spectrophotometer. The bleaching performance was monitored at contact times of

10, 20, 30, 40, 45, and 50 minutes. From Tables 5 and 6, it was seen that the absorbance and bleaching performance decreased and increased respectively as the dosage of adsorbent increased and as the time interval increased [14,3]. The relationships between the bleaching efficiency and the clay dosage variation at various contact times using the adsorbent are also shown in Fig. 7. The bleaching efficiency started to stabilize as the medium tended towards equilibrium [3]. The increase in bleaching efficiency remained constant for higher doses of adsorbent of up to 3 g but decreased in the rate at an adsorbent mass of 7 g. The highest bleaching performance at 3 g was 85.6% while that at 7 g was 78%. This could be because as the mass of the adsorbent was increased, the color pigments were completely adsorbed to the available active sites which blocked further adsorption and reduced the efficiency of the beaching performance [14,6].
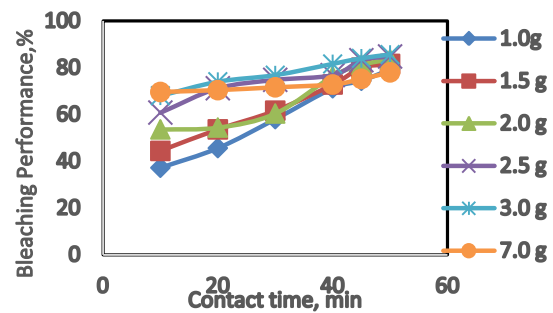

Fig. 7. Effect of adsorbent dosage on the bleaching efficiency of ACAC on palm oil

Table 3. Absorbance reading for ACAC from adsorption kinetics studies

Time (min)	Absorbance reading			
	50 °C	70 °C	90 °C	100 °C
10	2.42	2.28	1.78	1.57
20	2.38	2.20	1.54	1.38
30	2.35	1.86	1.28	1.02
40	2.33	1.82	1.25	0.74
45	2.32	1.78	1.21	0.66
50	2.31	1.76	1.16	0.53

Table 4. Bleaching performance for ACAC from adsorption kinetics studies

Time (min)	Bleaching performance (%)			
	50 °C	70 °C	90 °C	100 °C
10	3.2	8.8	28.8	37.2
20	4.8	12	38.4	44.8
30	6	25.6	48.8	59.2
40	6.8	27.2	50	70.4
45	7.2	28.8	51.6	73.6
50	7.6	29.6	53.6	78.8

Table 5. Absorbance reading for ACAC from equilibrium adsorption studies @ 100 °C

Time (min)	Absorbance					
	1 g	**1.5 g**	**2.0 g**	**2.5 g**	**3 g**	**7g**
10	1.57	1.39	1.16	0.98	0.80	0.76
20	1.36	1.16	1.14	0.72	0.65	0.74
30	1.05	0.96	0.99	0.63	0.58	0.71
40	0.72	0.68	0.59	0.58	0.46	0.68
45	0.64	0.50	0.47	0.42	0.40	0.62
50	0.52	0.46	0.41	0.38	0.36	0.55

Table 6. Bleaching performance for ACAC from equilibrium adsorption studies @ 100 °C

Time (min)	Bleaching performance (%)					
	1 g	**1.5 g**	**2.0 g**	**2.5 g**	**3 g**	**7g**
10	37.2	44.4	53.6	60.8	68.0	69.6
20	45.6	53.6	54.4	71.2	74.0	70.4
30	58.0	61.6	60.4	74.8	76.8	71.6
40	71.2	72.8	76.4	76.8	81.6	72.8
45	74.4	80.0	81.2	83.2	84.0	75.2
50	79.2	81.6	83.6	84.8	85.6	78.0

3.3 Adsorption Kinetic Modelling of Palm Oil Bleaching by ACAC

Kinetic modeling of beta-carotene adsorption can be used to analyze the performance of the adsorption process [9]. The efficiency of the adsorption rate can be obtained from the kinetic model plots where the rate of a reaction involving the mechanism and speed of the solute uptake are obtained [11,10]. The kinetic plots of the four models were used for the determination of the correlation coefficients and constants which act as a performance indicator of each model. The calculated kinetic constants and correlation coefficients at four different temperatures were presented in Table 7 while the kinetic plots are shown in Figs. 8-11. The kinetic model equations are shown in Table 8. The First-order kinetic model was investigated and low values of correlation coefficients (<0.9) were obtained. This showed that the modeling of the bleaching process of crude palm oil could not be described by the first-order kinetic model [11]. The pseudo-first-order kinetic model gave high values of correlation coefficients (>0.9) at all temperatures indicating good correlation showing that the modeling of the crude palm oil bleaching could be described by the model [10]. However, some researchers have obtained a low correlation coefficient (<0.9) from modeling with the pseudo-first-order model [11].

The plots of t/q_e versus time at the varying bleaching temperatures were utilized in the study of the application of the pseudo-second-order in describing the process. High values of correlation coefficients were obtained showing that the modeling of the crude palm oil bleaching could be described by the model except at the temperature of 70 °C. The adsorption capacities calculated in the pseudo-first-order model were higher than that calculated from the pseudo-second-order. The most commonly applied model for the identification of the adsorption process mechanism is the intra-particle diffusion model which expresses the relationship between the adsorption capacity (q_t) at time $t^{1/2}$. This model checks the likelihood of the adsorbate molecule diffusion from the surface of the adsorbent into the adsorbent pores [10]. "The correlation coefficients obtained from the kinetic model were high (>0.9 in most cases) indicating the suitability of the model in describing the kinetics of the removal of beta-carotene in crude palm oil. The linear plot of q_t versus $t^{1/2}$ did not pass through the origin indicating that the intra-particle diffusion is not the sole rate-limiting step for describing the kinetic process" [13,10]. "The boundary layer has some level of control if the plots do not pass through the origin, showing that other kinetic models may also control the rate of adsorption rate which may be operating simultaneously with the intra-particle diffusion model" [8,13].

The highest value of rate constant for the first-order, pseudo-first-order, pseudo-second-order and intra-particle diffusion models were at 70, 70, 100 and 100 °C respectively as 0.0320 min^{-1}, 0.0927 min^{-1}, 21.8561 g/mg min and 0.0963

mg/g min$^{1/2}$ (Table 7). The comparison of the analyzed data based on the correlation coefficient values showed that the experimental data were best described by the pseudo-first-order kinetic model as all the R^2 values were closest to 1.0 (>0.9) for all the varying temperatures [3]. The intraparticle diffusion model can also be applied in explaining the mechanism for the adsorption process.
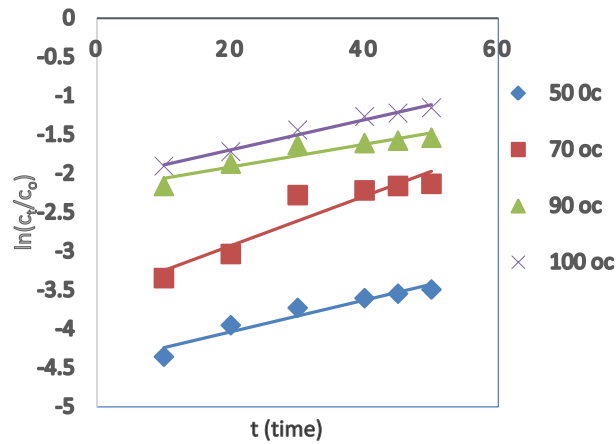

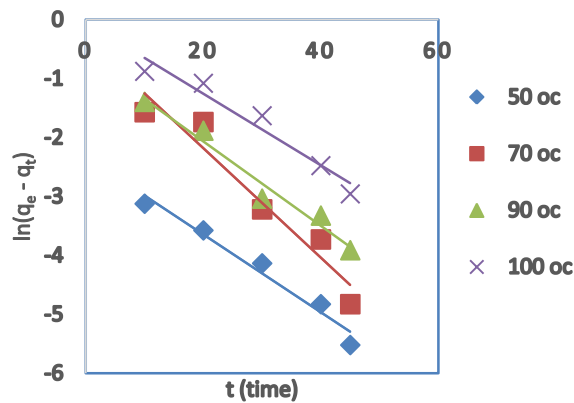**Fig. 8. Plot of First-order kinetic model**

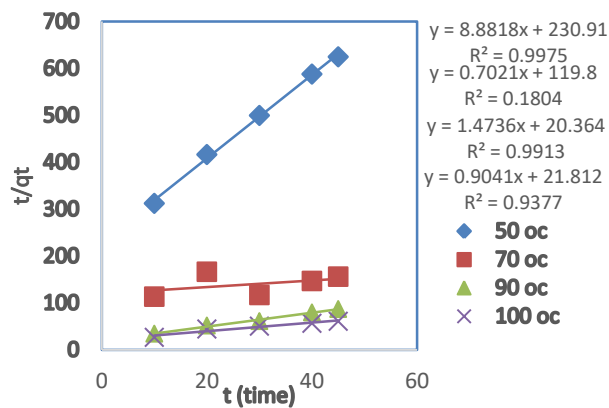**Fig. 9. Plot of Pseudo first-order kinetic model**

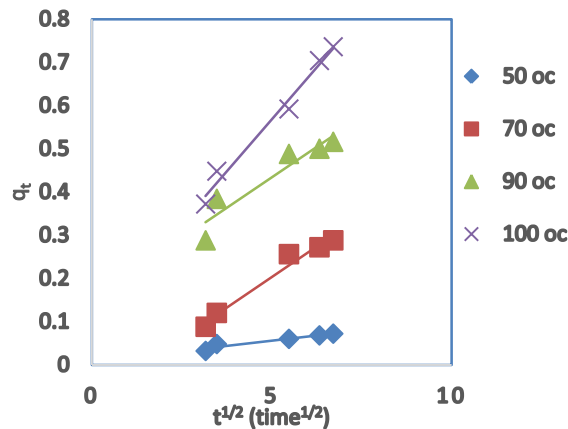**Fig. 10. Plot of Pseudo second-order kinetic model**

Fig. 11. Plot of Intra-particle diffusion kinetic model

Table 7. Adsorption kinetic parameters for the bleaching of palm oil using ACAC

Kinetic model	Kinetic constants	Temperature (^oC)			
		50	70	90	100
First-order	K (min^{-1})	0.0205	0.0320	0.0146	0.0193
	R^2	0.9304	0.8814	0.8792	0.9824
Pseudo first-order	K_1 (min^{-1})	0.0659	0.0927	0.0716	0.0697
	q_{e_1} (mg/g)	0.0978	0.7204	0.5313	0.9586
	R^2	0.9667	0.9324	0.9693	0.9464
Pseudo second-order	K_2 (g/mg min)	6,089.22	20,674.99	20.3691	21.8561
	q_{e_2} (mg/g)	0.0043	0.0083	0.0491	0.0458
	R^2	0.9975	0.1804	0.9913	0.9377
Intra-particle diffusion	K_d	0.0096	0.0565	0.0564	0.0963
	ε	0.0079	-0.0795	0.1518	0.086
	R^2	0.919	0.9719	0.8911	0.9834

Table 8. Kinetic equations of the adsorption models

Kinetic model	Parameter	Temperature (^oC)			
		50	70	90	100
First-order	Equation	y = 0.0205x - 4.4457	y = 0.032x - 3.5682	y = 0.0146x - 2.2083	y = 0.0193x - 2.0801
	R^2	R² = 0.9304	R² = 0.8814	R² = 0.8792	R² = 0.9824
Pseudo first-order	Equation	y = -0.0659x - 2.3249	y = -0.0927x - 0.328	y = -0.0716x - 0.6325	y = -0.0607x - 0.0423
	R^2	R² = 0.9667	R² = 0.9324	R² = 0.9693	R² = 0.9464
Pseudo second-order	Equation	y = 8.8818x + 230.91	y = 0.7021x + 119.8	y = 1.4736x + 20.364	y = 0.9041x + 21.812
	R^2	R² = 0.9975	R² = 0.1804	R² = 0.9913	R² = 0.9377
Intra-particle diffusion	Equation	y = 0.0096x + 0.0079	y = 0.0565x - 0.0795	y = 0.0564x + 0.1518	y = 0.0963x + 0.086
	R^2	R² = 0.919	R² = 0.9719	R² = 0.8911	R² = 0.9834

3.4 Equilibrium Kinetic Modelling of Palm Oil Bleaching by ACAC

The fitness of the Langmuir, Freundlich, and Temkin isotherm models at varying temperatures were investigated and the evaluated constants and coefficient of correlation (R^2) were listed in Table 9. Their linear plots at varying temperatures were not shown due to cumbersomeness. The coefficient of correlation

was applied in the prediction of the model fitness. The value of q_m measured the surface area of the clay while the positive value of K_1 indicated that the adsorbent was good for the adsorption of carotene in crude palm oil [27]. The decreasing value of the adsorption rate (K_1) with temperature (negative correlation) indicated the decrease in the affinity between adsorbent and adsorbate as the temperature increased [12]. The maximum adsorptive capacity (q_m) increased with increasing temperature showing that the adsorption process was an endothermic one [12]. However, the value of q_m obtained was lower than observed in other researches [11-12,28]. The value of q_m obtained in this work is comparable to the value reported by [13,29-31] where low values of q_m (≤ 2) were also obtained after evaluation. This indicated that the adsorption capacity of beta carotene on ACAC was lesser when compared to other clays. However, [12] highlighted that the study of adsorption in a narrow liquid concentration may overestimate the monolayer capacity. The R^2 values from Langmuir modeling were high (>0.9) and may have been due to a homogeneous distribution of active sites on the activated clay [10].

The constant K in the Freundlich isotherm model measures the adsorption capacity while constant n is a measured the favorability and intensity of the adsorption process [11]. The adsorptive capacity (K) increased with temperature up to the maximum temperature of 100 ^{o}C applied, indicating an endothermic adsorption process and favorability at high temperatures [11,12]. [11,10] stated that beneficial adsorption of beta carotene required that the value of n should lie between 1 and 10. However, from Table 8, it was seen that the values of n at four different temperatures were <1 [14-15]. The negative value of n obtained could be attributed to a high degree of carotene adsorption to the ACAC adsorbent used and the surface heterogeneity of its active sites [15]. The values of R^2 from the four isotherm models were quite high, with Langmuir, Freundlich, and Temkin isotherms having R^2 values >0.9. This is an indication that the data for the bleaching of crude palm oil with ACAC could be fitted to all the models as also observed in [15]. However, according to the correlation coefficient, the data were slightly better fitted by the Temkin model than the Freundlich and Langmuir models respectively as also reported by [14-15]. This indicated that the surface of ACAC was heterogeneous [15].

3.5 Adsorption Thermodynamics

The thermodynamic plot and values of ΔG^o, ΔH^o and ΔS^o are shown in Fig. 12 and Table 10 respectively. The value of ΔH^o was positive as obtained by [14,12,10,3]. This indicates the endothermic nature of the adsorptive bleaching of crude palm oil on ACAC between 343 - 373 K temperatures [14]. This explains that more heat (energy) is required as the reaction proceeds to improve adsorption because the total energy released in the bond making is less than the total energy absorbed in bond breaking between the adsorbent and adsorbate [10]. This also indicates that the adsorption of beta carotene on ACAC took place via chemisorption (chemical adsorption process) since it was an endothermic process as physisorption is always exothermic. This result was in agreement with a researcher who reported that β-carotenes are mostly chemisorbed onto acid-activated bleaching clays [12]. However, some researchers reported that the value of enthalpy change indicated the type of adsorption, as the physical adsorption process gave a heat change of between 2.1 to 20.9 kJ/mol while chemical adsorption obtained about 80 to 200 kJ/mol of heat [15].

Table 9. Equilibrium isotherm parameters for the bleaching of palm oil using ACAC

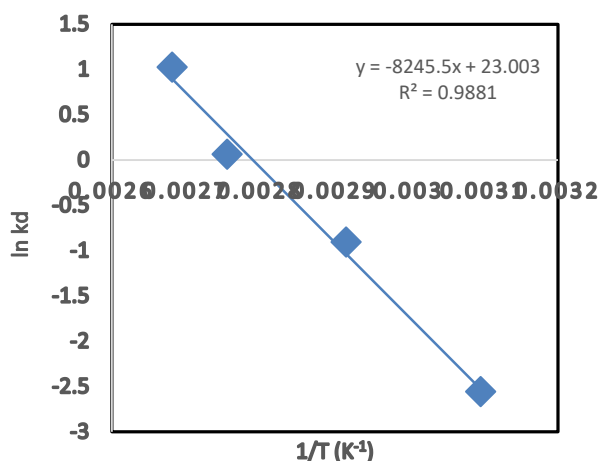| Adsorption isotherm model	Kinetic constants	Temperature (^{o}C)			
		50	70	90	100
Langmuir	K_1 (l/mg)	0.8972	0.6500	0.3414	0.1607
	q_m (mg/g)	0.0028	0.0426	0.4579	1.8646
	R^2	0.9464	0.9602	0.9779	0.9681
Freundlich	K (l/g)	4.06×10^{-19}	2.59×10^{-5}	0.0363	0.2075
	n	-0.5768	-0.8290	-1.3550	-1.8801
	R^2	0.9844	0.9872	0.9844	0.9515
Temkin	K_T (mg/g)	0.9985	0.9805	0.8464	0.0963
	b (KJ/mol)	-2.8396	-3.5460	-5.210	8.0444
	R^2	1.0	0.9996	0.9974	0.9819

Fig. 12. Thermodynamics plot of crude palm oil bleaching with ACAC

Table 10. Thermodynamic parameters for adsorption of beta carotene onto ACAC

Temperature (K)	Thermodynamic properties		
	ΔG^{o} (J/mol)	ΔH (J/mol)	ΔS (J/mol)
323	6,780.3413	68,553.09	191.2469
343	2,955.4033		
363	-869.5347		
373	-2,782.0037		

The positive value obtained from entropy evaluation showed that process was feasible and did not go against the second law of thermodynamics [24]. The positive value of entropy also suggested an increase in randomness at the solid/liquid interface during adsorption [14,3]. This was because the number of water molecules surrounding the adsorbate was reduced during the process of bleaching thereby increasing the degree of freedom of the water molecules and the randomness at the solid/liquid interface during adsorption [10]. The positive values of ΔG^{o} obtained at 323 and 343 K implied that the adsorption of beta carotene onto ACAC was not spontaneous at lower temperatures [24]. Negative ΔG^{o} values indicated spontaneous reactions [10]. Hence, bleaching at higher temperatures of 363 and 373 K led to spontaneous reactions. The negative values of ΔG^{o} as temperature increased indicated that the adsorption was more favorable at higher temperatures [18]. [19] obtained negative values of ΔG at higher temperatures and reported that the adsorption was unfavorable at a higher temperature. [3] also reported the decrease in ΔG values with increasing temperature showing that the feasibility of adsorption increased at higher temperatures.

4. CONCLUSION

Achalla clay activated with hydrochloric acid has been identified as an efficient adsorbent for beta carotene removal from crude palm oil, with up to 85.6% removal at 100 ^{o}C. Characterization of the raw and activated clays with XRF, SEM, and FTIR indicated that the clays were kaolinites with some major changes after activation which were observed from the significant increase in the number of microporous surfaces and some changes in the functional groups. Adsorption of beta carotene onto the clay surfaces increased with temperature, adsorbent dosage, and contact time. The maximum experimental bleaching efficiency was recorded at 3 g of the clay dosage. Kinetic studies revealed that equilibrium was reached within 50 minutes. The adsorption mechanism studies indicated that the intra-particle diffusion was not the sole determinant of the mechanism of the bleaching process as the pseudo-first-order model described the adsorption process from the experimental data with higher correlation coefficients than other kinetic models. The adsorption isotherm studies showed that the Temkin isotherm better explained the experimental data for the bleaching of crude palm oil using acid-activated Achalla

clay than Langmuir and Freundlich isotherms with the R^2 values of Temkin isotherm ranging between 0.9819 to 1.0, while the Langmuir and Freundlich isotherm gave a lesser fit. The thermodynamic parameters (ΔH, ΔS, and ΔG) showed that the adsorptive bleaching process was spontaneous and an endothermic one as a higher temperature was more favorable, with increasing randomness at the solid/solution interface. Its endothermic nature showed that the adsorption of beta carotene on the activated clay was a chemical adsorption process (chemisorption). Hence, Achalla clay from Anambra state, Nigeria can be used as an economically potential adsorbent for the bleaching of crude palm oil.

COMPETING INTERESTS

The authors have declared that no competing interests exist.

REFERENCES

1. Ojewumi ME, Ehinmowo AB, Obanla OR, Durodola BM, Ezeocha RC. Comparative analysis on the bleaching of crude palm oil using activated groundnut hull, snail shell and rice husk. Heliyon. 2021;7(e07747):1-16. DOI:https://doi.org/10.1016/j.heliyon.2021.e07747.
2. Yuliana M, Sutrisno RJ, Hermanto S, Ismadji S, Wijaya CJ, Santoso SP. et al. Hydrophobic cetyltrimethylammonium bromide-pillared bentonite as an effective palm oil bleaching agent. ACS Omega. 2020;5:28844-28855.
3. Usman MA, Oribayo A, Adebayo AA. Bleaching of palm oil by activated local bentonite and kaolin clay from afashio, Edo-Nigeria. Chem Process Eng Res. 2013;10:1-13.
4. Bayram H, Ustunisik G, Önal M, Sarıkaya Y. Optimization of bleaching power by sulfuric acid activation of bentonite. Clay Minerals. 2021;56:148-155. DOI:https://doi.org/10.1180/clm.2021.28.
5. Salawudeen TO, Arinkoola AO, Jimoh MO, Akinwande BA. Clay characterization and optimisation of bleaching parameters for palm kernel oil using alkaline activated clays. J Miner Mat Charact Eng. 2014;2:586-597.
6. Ajemba RO, Igbokwe PK Onukwuli OD. Optimization of color pigments removal from palm oil by activated Ukpor clay using response surface methodology. Res J Appl Sci, Eng Technol. 2013;6(3):423-432.
7. Mustapha SI, Mohammed AA, Zakari AY, Mohammed HA. Performance evaluation of local clays from northern Nigeria for the refining of palm oil. J Chem Eng Mat Sci. 2013;4(5):58-66.
8. Jasper EE, Ajibola VO, Onwuka JC. Nonlinear regression analysis of the sorption of crystal violet and methylene blue from aqueous solutions onto an agro- waste derived activated carbon. Appl Wat Sci. 2020;10(132):1-11. DOI:https://doi.org/10.1007/s13201-020-01218-y.
9. Permana T, Noor E, Arkeman Y. Evaluation of kinetic models of Beta-carotene adsorption from palm oil onto bentonite. Int J Sci Technol. Res. 2018;7(4):23-31.
10. Nwabanne JT, Onu CE, Nwankwoukwu OC. Equilibrium, kinetics and thermodynamics of the bleaching of palm oil using activated Nando clay. J Eng Res Rep. 2018;1(3):1-13.
11. Asadu CO, Ezema CA, Onu CE, Ike IS, Onoghwarite OE, Umeagukwu EO. Development of an adsorbent for the remediation of crude oil polluted water using stearic acid grafted coconut husk (Cocos nucifera) composite. Appl Surf Sci Adv. 2021;6(100179):1-18. DOI:https://doi.org/10.1016/j.apsadv.2021.100179.
12. Almeida ES, Carvalho ACB, Soares IO, Valadares LF, Mendonça ARV, Ivanildo JS. et al. Elucidating how two different types of bleaching earths widely used in vegetable oils industry remove carotenes from palm oil: Equilibrium, kinetics and thermodynamic parameters. Food Res Int. 2019;121:785–797.
13. Nnanwube IA, Onukwuli OD, Okafor VN, Obibuenyi JI, Ajemba RO, Chukwuka CC. Equilibrium, Kinetics and Optimization Studies on the Bleaching of Palm Oil Using Activated Karaworo Kaolinite. J. Mater. Environ. Sci. 2019;11(10):1599-1615.
14. Okafor VN, Nnanwube IA, Obibuenyi JI, Onukwuli OD, Ajemba RO. Removal of pigments from palm oil using activated Ibusa kaolinite: Equilibrium, kinetic and thermodynamic studies. J Miner Mat Charact Eng. 2019;7:157-170.
15. Chairgulprasert, V, Madlah P. Removal of Free Fatty Acid from Used Palm Oil by

Coffee Husk Ash. Sci Technol Asia. 2018;23(3):1-9.
DOI: 10.14456/scitechasia.2018.18.

16. Silva SM, Sampaio KA, Ceriani R, Verhé R, Stevens C, De Greyt W. et al. Adsorption of carotenes and phosphorus from palm oil onto acid activated bleaching earth: Equilibrium, kinetics and thermodynamics. J Food Eng. 2013;118:341-349.

17. Piccin JS, Dotto GL, Pinto LAA. Adsorption isotherms and thermochemical data of FD&C RED^o 40 binding by chitosan. Brazil J Chem Eng. 2011;28(02):295-304.

18. Nandiyanto ABD, Oktiani R, Ragadhita R. How to read and interpret FTIR spectroscope of organic material. J Sci Technol. 2019;4(1):97-118.

19. Stuart BH. Infrared Spectroscopy: Fundamentals and Applications. John Wiley & Sons, Ltd, 1st Ed., 2004;208 pages. ISBNs: 0-470-85427-8 (HB); 0-470-85428-6 (PB).

20. Coates J. Interpretation of Infrared Spectra, A Practical Approach. Encyclopedia of Analytical Chemistry, R.A. Meyers (Ed.). 2000;10815–10837. Ó John Wiley & Sons Ltd, Chichester.

21. Chen Y, Zou C, Mastalerz M, Hu S, Gasaway C, Tao, X. Applications of Micro-Fourier Transform Infrared Spectroscopy (FTIR) in the Geological Sciences - A Review. Int J Mol Sci. 2015;16:30223–30250.

22. Djomgoue, P, Njopwouo D. FT-IR spectroscopy applied for surface clays characterization. J Surf Eng Mat Adv Technol. 2013;3:275-282.
DOI:http://dx.doi.org/10.4236/jsemat.2013.34037.

23. Diko M, Ekosse G, Ogola J. Fourier transform infrared spectroscopy and thermal analyses of kaolinitic clays from South Africa and Cameroon. Acta Geod Geomat. 2016;13(2):182:xx1–x10.

DOI: 10.13168/AGG.2015.0052.

24. Thompson CO, Ndukwe AO, Asadu CO. Application of activated biomass waste as an adsorbent for the removal of lead (II) ion from wastewater. Emerg Contam. 2020;6:259-267.

25. Oli SC, Kamalu CIO, Obijiaku JC, Opebiyi SO, Oghome P, Nkwocha AC. A study on the bleaching properties of locally sourced clay (Ukpor clay) for the processing of palm oil. Int J Mod Res in Eng Technol. (IJMRET). 2017;2(5):14-29.

26. Uddin F. Clay, nanoclays and montmorillonite minerals. The Miner Met Mat Soc and ASM Int. 2008.
DOI: 10.1007/s11661-008-9603-5.

27. Nwabanne JT, Ekwu CE. Decolourization of palm oil by Nigerian local clay: A study of adsorption isotherms and bleaching kinetics. Int J Mult Sci Eng. 2013;4(1):20-25.

28. Popoola, L.T. Characterization and adsorptive behaviour of snail shell-rice husk (SS-RH) calcined particles (CPs) towards cationic dye. Heliyon. 2019; 5(2019):e01153.
DOI: 10.1016/j.heliyon.2019,e01153.

29. Nweke CN, Ajemba RO. Clay characterization and bleaching of crude palm oil using acid-activated Nibo clay. Biorem. Sci. Technol. Res. 2022;10(1):14-21.

30. Anyikwa SO, Nwakaudu MS, Nzeoma C, Yakubu E. Kinetics and equilibrium studies of colour pigments removal from crude palm oil using acid activated kaolin clay and mathematical method. Int. J. Sci. Eng. Inves. 2021;10(116):30-44.

31. Mukasa-Tebandeke IZ, Wasajja-Navayojo ZH, Ssebuwufu PJM, Wasswa J, Nankinga, R, Lugolobi F, Schumann A. How variation of turbidity of bleached oils characterizes purity oil and bleaching processes. Int. J. Adv. Res. Chem. Sci. 2017;4(5):36-65.

Peer-review history:
The peer review history for this paper can be accessed here:
https://www.sdiarticle5.com/review-history/96393